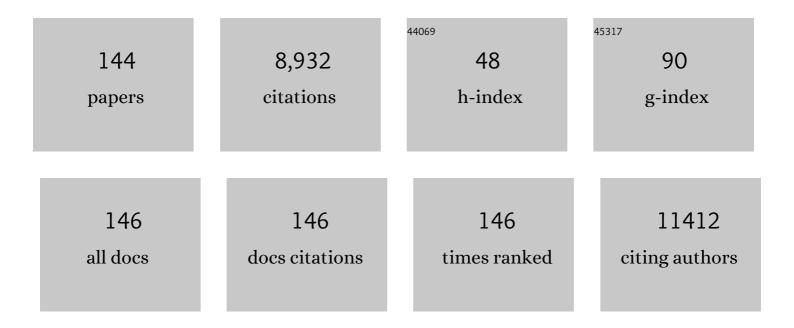
List of Publications by Year in descending order

Source: https://exaly.com/author-pdf/2596159/publications.pdf Version: 2024-02-01



SHI-7F YANG

#	Article	IF	CITATIONS
1	Ultrasound-driven fabrication of high-entropy alloy nanocatalysts promoted by alcoholic ionic liquids. Nano Research, 2022, 15, 4792-4798.	10.4	13
2	Reaching the Excitonic Limit in 2D Janus Monolayers by In Situ Deterministic Growth. Advanced Materials, 2022, 34, e2106222.	21.0	39
3	Sublayer-enhanced atomic sites of single atom catalysts through <i>in situ</i> atomization of metal oxide nanoparticles. Energy and Environmental Science, 2022, 15, 1183-1191.	30.8	25
4	Construction of single-atom catalysts for electro-, photo- and photoelectro-catalytic applications: State-of-the-art, opportunities, and challenges. Materials Today, 2022, 53, 217-237.	14.2	34
5	Reaching the Excitonic Limit in 2D Janus Monolayers by In Situ Deterministic Growth (Adv. Mater.) Tj ETQq1 1 C	0.784314 rg 21.0	gBT ₀ /Overloci
6	Observation of Cobalt Species Evolution in Mesoporous Carbon by Inâ€Situ STEMâ€HAADF Imaging and Related Hydrogenation Process. ChemistrySelect, 2022, 7, .	1.5	0
7	<scp>Lowâ€ŧemperature</scp> total oxidation of methane by pore―and vacancyâ€engineered <scp>NiO</scp> catalysts. AICHE Journal, 2022, 68, .	3.6	10
8	Carbon allotropes form a hybrid material: Synthesis, characterization, and molecular dynamics simulation of novel graphene-glassy carbon hybrid material. Carbon, 2022, 196, 1012-1023.	10.3	4
9	First demonstration of phosphate enhanced atomically dispersed bimetallic FeCu catalysts as Pt-free cathodes for high temperature phosphoric acid doped polybenzimidazole fuel cells. Applied Catalysis B: Environmental, 2021, 284, 119717.	20.2	28
10	Designed Iron Single Atom Catalysts for Highly Efficient Oxygen Reduction Reaction in Alkaline and Acid Media. Advanced Materials Interfaces, 2021, 8, 2001788.	3.7	11
11	Sulphur as medium: Directly converting pitch into porous carbon. Fuel, 2021, 286, 119393.	6.4	17
12	Coupling hydrothermal and photothermal single-atom catalysis toward excellent water splitting to hydrogen. Applied Catalysis B: Environmental, 2021, 283, 119660.	20.2	77
13	A template-free method to synthesis high density iron single atoms anchored on carbon nanotubes for high temperature polymer electrolyte membrane fuel cells. Nano Energy, 2021, 80, 105534.	16.0	35
14	<scp>Entropyâ€stabilized metal eO_{<i>x</i>}</scp> solid solutions for catalytic combustion of volatile organic compounds. AICHE Journal, 2021, 67, .	3.6	30
15	Cobalt Single Atoms Embedded in Nitrogenâ€Doped Graphene for Selective Oxidation of Benzyl Alcohol by Activated Peroxymonosulfate. Small, 2021, 17, e2004579.	10.0	47
16	Perovskite Oxide–Halide Solid Solutions: A Platform for Electrocatalysts. Angewandte Chemie, 2021, 133, 10041-10046.	2.0	3
17	Thermodynamics of order and randomness in dopant distributions inferred from atomically resolved imaging. Npj Computational Materials, 2021, 7, .	8.7	1
18	Perovskite Oxide–Halide Solid Solutions: A Platform for Electrocatalysts. Angewandte Chemie - International Edition, 2021, 60, 9953-9958.	13.8	26

#	Article	IF	CITATIONS
19	Investigating phase transitions from local crystallographic analysis based on statistical learning of atomic environments in 2D MoS2-ReS2. Applied Physics Reviews, 2021, 8, 011409.	11.3	7
20	Mechanochemical Redox: Calcinationâ€free Synthesis of Ceriaâ€hybrid Catalyst with Ultraâ€High Surface Area. ChemCatChem, 2021, 13, 2434-2443.	3.7	4
21	Tensile behavior and inelastic strain recovery of Cu-Co nanolaminates. Scripta Materialia, 2021, 197, 113781.	5.2	4
22	Photoinduced Strong Metal–Support Interaction for Enhanced Catalysis. Journal of the American Chemical Society, 2021, 143, 8521-8526.	13.7	85
23	Local and Bulk Probe of Vanadium-Substituted α-Manganese Oxide (α-K <i>_x</i> V <i>_y</i> Mn _{8–<i>y</i>} O ₁₆) Lithium Electrochemistry. Inorganic Chemistry, 2021, 60, 10398-10414.	4.0	3
24	Entropy-driven chemistry reveals highly stable denary MgAl2O4-type catalysts. Chem Catalysis, 2021, 1, 648-662.	6.1	31
25	Exsolution–Dissolution of Supported Metals on High-Entropy Co ₃ MnNiCuZnO <i>_x</i> : Toward Sintering-Resistant Catalysis. ACS Catalysis, 2021, 11, 12247-12257.	11.2	39
26	Atomically dispersed cobalt on graphitic carbon nitride as a robust catalyst for selective oxidation of ethylbenzene by peroxymonosulfate. Journal of Materials Chemistry A, 2021, 9, 3029-3035.	10.3	48
27	Coordination tailoring of Cu single sites on C3N4 realizes selective CO2 hydrogenation at low temperature. Nature Communications, 2021, 12, 6022.	12.8	132
28	Iridium metallene oxide for acidic oxygen evolution catalysis. Nature Communications, 2021, 12, 6007.	12.8	137
29	Spontaneous amorphous oxide-interfaced ultrafine noble metal nanoclusters for unexpected anodic electrocatalysis. Chem Catalysis, 2021, 1, 1104-1117.	6.1	14
30	A Universal Seeding Strategy to Synthesize Single Atom Catalysts on 2D Materials for Electrocatalytic Applications. Advanced Functional Materials, 2020, 30, 1906157.	14.9	91
31	Roomâ€Temperature Synthesis of Highâ€Entropy Perovskite Oxide Nanoparticle Catalysts through Ultrasonicationâ€Based Method. ChemSusChem, 2020, 13, 111-115.	6.8	104
32	Atomically Dispersed Pd Supported on Zinc Oxide for Selective Nonoxidative Ethanol Dehydrogenation. Industrial & Engineering Chemistry Research, 2020, 59, 2648-2656.	3.7	29
33	Theoretical Calculation Guided Design of Single-Atom Catalysts toward Fast Kinetic and Long-Life Li–S Batteries. Nano Letters, 2020, 20, 1252-1261.	9.1	394
34	On-Demand, Ultraselective Hydrogenation System Enabled by Precisely Modulated Pd–Cd Nanocubes. Journal of the American Chemical Society, 2020, 142, 962-972.	13.7	53
35	Deep Understanding of Strong Metal Interface Confinement: A Journey of Pd/FeO _{<i>x</i>} Catalysts. ACS Catalysis, 2020, 10, 8950-8959.	11.2	113
36	Self-regenerative noble metal catalysts supported on high-entropy oxides. Chemical Communications, 2020, 56, 15056-15059.	4.1	34

#	Article	IF	CITATIONS
37	Mechanochemical redox: a calcination-free process to support CoMnO _x catalysts. Catalysis Science and Technology, 2020, 10, 6525-6532.	4.1	1
38	Stable and Catalytically Active Shape-Engineered Cerium Oxide Nanorods by Controlled Doping of Aluminum Cations. ACS Applied Materials & amp; Interfaces, 2020, 12, 37774-37783.	8.0	6
39	Scanning Transmission Electron Microscopy (STEM) Study on Novel Two-dimensional Materials. Microscopy and Microanalysis, 2020, 26, 2372-2374.	0.4	0
40	Sinter-Resistant Nanoparticle Catalysts Achieved by 2D Boron Nitride-Based Strong Metal–Support Interactions: A New Twist on an Old Story. ACS Central Science, 2020, 6, 1617-1627.	11.3	42
41	Singleâ€Atom Inâ€Doped Subnanometer Pt Nanowires for Simultaneous Hydrogen Generation and Biomass Upgrading. Advanced Functional Materials, 2020, 30, 2004310.	14.9	77
42	The Effects of Vanadium Substitution on One-dimensional Tunnel Structures of Cryptomelane: Combined TEM and DFT Study. Microscopy and Microanalysis, 2020, 26, 3162-3164.	0.4	0
43	Atomic Electron Tomography: Past, Present and Future. Microscopy and Microanalysis, 2020, 26, 652-654.	0.4	1
44	Roomâ€Temperature Synthesis of 2D Janus Crystals and their Heterostructures. Advanced Materials, 2020, 32, e2006320.	21.0	138
45	A Principle for Highly Active Metal Oxide Catalysts via NaCl-Based Solid Solution. CheM, 2020, 6, 1723-1741.	11.7	30
46	Three-Dimensional Patterning of Nanoparticles by Molecular Stamping. ACS Nano, 2020, 14, 6823-6833.	14.6	42
47	Valence-programmable nanoparticle architectures. Nature Communications, 2020, 11, 2279.	12.8	37
48	Mechanochemical redox-based synthesis of highly porous Co Mn1-O catalysts for total oxidation. Chinese Journal of Catalysis, 2020, 41, 1846-1854.	14.0	15
49	Revealing the role of oxygen vacancies in bimetallic PbBiO2Br atomic layers for boosting photocatalytic CO2 conversion. Applied Catalysis B: Environmental, 2020, 277, 119170.	20.2	77
50	Harnessing strong metal–support interactions via a reverse route. Nature Communications, 2020, 11, 3042.	12.8	84
51	High-loading single Pt atom sites [Pt-O(OH) <i> _x </i>] catalyze the CO PROX reaction with high activity and selectivity at mild conditions. Science Advances, 2020, 6, eaba3809.	10.3	78
52	Cation Exchange Strategy to Single-Atom Noble-Metal Doped CuO Nanowire Arrays with Ultralow Overpotential for H ₂ O Splitting. Nano Letters, 2020, 20, 5482-5489.	9.1	93
53	Boosting electrosynthesis of ammonia on surface-engineered MXene Ti3C2. Nano Energy, 2020, 72, 104681.	16.0	82
54	Solvent-free synthesis of mesoporous platinum-aluminum oxide via mechanochemistry: Toward selective hydrogenation of nitrobenzene to aniline. Chemical Engineering Science, 2020, 220, 115619.	3.8	29

#	Article	IF	CITATIONS
55	Correlating the three-dimensional atomic defects and electronic properties of two-dimensional transition metal dichalcogenides. Nature Materials, 2020, 19, 867-873.	27.5	96
56	Vanadium-Substituted Tunnel Structured Silver Hollandite (Ag _{1.2} V _{<i>x</i>} Mn _{8–<i>x</i>} O ₁₆): Impact on Morphology and Electrochemistry. Inorganic Chemistry, 2020, 59, 3783-3793.	4.0	4
57	The effects of vanadium substitution on one-dimensional tunnel structures of cryptomelane: Combined TEM and DFT study. Nano Energy, 2020, 71, 104571.	16.0	11
58	Atomic defects in ultra-thin mesoporous TiO2 enhance photocatalytic hydrogen evolution from water splitting. Applied Surface Science, 2020, 513, 145723.	6.1	37
59	New Insights into the Reaction Mechanism of Sodium Vanadate for an Aqueous Zn Ion Battery. Chemistry of Materials, 2020, 32, 2053-2060.	6.7	37
60	Controlled Oneâ€pot Synthesis of Nickel Single Atoms Embedded in Carbon Nanotube and Graphene Supports with High Loading. ChemNanoMat, 2020, 6, 1063-1074.	2.8	14
61	Effects of Surface Terminations of 2D Bi ₂ WO ₆ on Photocatalytic Hydrogen Evolution from Water Splitting. ACS Applied Materials & Interfaces, 2020, 12, 20067-20074.	8.0	78
62	Facile benzene reduction promoted by a synergistically coupled Cu–Co–Ce ternary mixed oxide. Chemical Science, 2020, 11, 5766-5771.	7.4	8
63	Detection of defects in atomic-resolution images of materials using cycle analysis. Advanced Structural and Chemical Imaging, 2020, 6, .	4.0	11
64	Homogeneous superconducting gap in <mml:math xmlns:mml="http://www.w3.org/1998/Math/MathML"><mml:mrow><mml:mi>Dy</mml:mi><mml:msub><mml:n mathvariant="normal">O<mml:mrow><mml:mn>7</mml:mn><mml:mo>â^'</mml:mo><mml:mi>δsynthesized by oxide molecular beam epitaxy. Physical Review Materials, 2020, 4, .</mml:mi></mml:mrow></mml:n </mml:msub></mml:mrow></mml:math 	ni>Banml:mi> </td <td>ml:mi> < mml:r mml:mrow> <!--</td--></td>	ml:mi> < mml:r mml:mrow> </td
65	In Situ Visualization of Structural Evolution and Fissure Breathing in (De)lithiated H ₂ V ₃ O ₈ Nanorods. ACS Energy Letters, 2019, 4, 2081-2090.	17.4	19
66	Electronic Structure and Coupling of Re Clusters In Monolayer MoS2. Microscopy and Microanalysis, 2019, 25, 506-507.	0.4	0
67	Determining the 3D Atomic Coordinates and Crystal Defects in 2D Materials with Picometer Precision. Microscopy and Microanalysis, 2019, 25, 404-405.	0.4	1
68	Protecting the Nanoscale Properties of Ag Nanowires with a Solution-Grown SnO ₂ Monolayer as Corrosion Inhibitor. Journal of the American Chemical Society, 2019, 141, 13977-13986.	13.7	45
69	Statistical Physics-based Framework and Bayesian Inference for Model Selection and Uncertainty Quantification. Microscopy and Microanalysis, 2019, 25, 130-131.	0.4	3
70	Strong Effect of B-Site Substitution on the Reactivity of Layered Perovskite Oxides Probed via Isopropanol Conversion. , 2019, 1, 230-236.		10
71	Solvent-free and rapid synthesis of mesoporous Pt–iron oxide catalysts <i>via</i> mechanochemical assembly. Catalysis Science and Technology, 2019, 9, 3907-3913.	4.1	9
72	Isolated single atom cobalt in Bi3O4Br atomic layers to trigger efficient CO2 photoreduction. Nature Communications, 2019, 10, 2840.	12.8	327

#	Article	IF	CITATIONS
73	Mechanochemical Nonhydrolytic Sol–Gel-Strategy for the Production of Mesoporous Multimetallic Oxides. Chemistry of Materials, 2019, 31, 5529-5536.	6.7	65
74	Simultaneously Boosting the Ionic Conductivity and Mechanical Strength of Polymer Gel Electrolyte Membranes by Confining Ionic Liquids into Hollow Silica Nanocavities. Batteries and Supercaps, 2019, 2, 985-991.	4.7	21
75	Mechanochemical Synthesis of High Entropy Oxide Materials under Ambient Conditions: Dispersion of Catalysts via Entropy Maximization. , 2019, 1, 83-88.		143
76	Promoting Pt catalysis for CO oxidation <i>via</i> the Mott–Schottky effect. Nanoscale, 2019, 11, 18568-18574.	5.6	13
77	Atomic-level tunnel engineering of todorokite MnO2 for precise evaluation of lithium storage mechanisms by in situ transmission electron microscopy. Nano Energy, 2019, 63, 103840.	16.0	17
78	Atomically Dispersed Bimetallic FeNi Catalysts as Highly Efficient Bifunctional Catalysts for Reversible Oxygen Evolution and Oxygen Reduction Reactions. ChemElectroChem, 2019, 6, 3478-3487.	3.4	58
79	Defect-Mediated Phase Transformation in Anisotropic Two-Dimensional PdSe ₂ Crystals for Seamless Electrical Contacts. Journal of the American Chemical Society, 2019, 141, 8928-8936.	13.7	81
80	Defectâ€Tailoring Mediated Electron–Hole Separation in Singleâ€Unitâ€Cell Bi ₃ O ₄ Br Nanosheets for Boosting Photocatalytic Hydrogen Evolution and Nitrogen Fixation. Advanced Materials, 2019, 31, e1807576.	21.0	311
81	Optically manipulated nanomechanics of semiconductor nanowires. Chinese Physics B, 2019, 28, 054204.	1.4	5
82	Mechanochemical Synthesis of Ruthenium Cluster@Ordered Mesoporous Carbon Catalysts by Synergetic Dual Templates. Chemistry - A European Journal, 2019, 25, 8494-8498.	3.3	10
83	Reversibly tuning the surface state of Ag via the assistance of photocatalysis in Ag/BiOCl. Nanotechnology, 2019, 30, 305601.	2.6	16
84	Entropyâ€Maximized Synthesis of Multimetallic Nanoparticle Catalysts via a Ultrasonicationâ€Assisted Wet Chemistry Method under Ambient Conditions. Advanced Materials Interfaces, 2019, 6, 1900015.	3.7	130
85	Direct Cation Exchange in Monolayer <mml:math <br="" xmlns:mml="http://www.w3.org/1998/Math/MathML">display="inline"><mml:mrow><mml:msub><mml:mrow><mml:mi>MoS</mml:mi></mml:mrow><mml:mn>2via Recombination-Enhanced Migration. Physical Review Letters, 2019, 122, 106101.</mml:mn></mml:msub></mml:mrow></mml:math>	ˈml .7 181> <td>mnzlımsub><</td>	mn zlı msub><
86	Iron Single Atoms on Graphene as Nonprecious Metal Catalysts for Highâ€Temperature Polymer Electrolyte Membrane Fuel Cells. Advanced Science, 2019, 6, 1802066.	11.2	164
87	High-performance electrolytic oxygen evolution with a seamless armor core–shell FeCoNi oxynitride. Nanoscale, 2019, 11, 7239-7246.	5.6	28
88	Supported Single Atoms as New Class of Catalysts for Electrochemical Reduction of Carbon Dioxide. Small Methods, 2019, 3, 1800440.	8.6	155
89	Optimizing PtFe intermetallics for oxygen reduction reaction: from DFT screening to <i>in situ</i> XAFS characterization. Nanoscale, 2019, 11, 20301-20306.	5.6	33
90	Unsaturated edge-anchored Ni single atoms on porous microwave exfoliated graphene oxide for electrochemical CO2. Applied Catalysis B: Environmental, 2019, 243, 294-303.	20.2	243

#	Article	IF	CITATIONS
91	Designing a highly efficient polysulfide conversion catalyst with paramontroseite for high-performance and long-life lithium-sulfur batteries. Nano Energy, 2019, 57, 230-240.	16.0	190
92	Spatially controlled doping of two-dimensional SnS2 through intercalation for electronics. Nature Nanotechnology, 2018, 13, 294-299.	31.5	269
93	Ultraâ€Stable and Highâ€Cobaltâ€Loaded Cobalt@Ordered Mesoporous Carbon Catalysts: Allâ€inâ€One Deoxygenation of Ketone into Alkylbenzene. ChemCatChem, 2018, 10, 3299-3304.	3.7	17
94	Facile Synthesis of Highly Porous Metal Oxides by Mechanochemical Nanocasting. Chemistry of Materials, 2018, 30, 2924-2929.	6.7	54
95	High-Capacity and Long-Cycle Life Aqueous Rechargeable Lithium-Ion Battery with the FePO ₄ Anode. ACS Applied Materials & Interfaces, 2018, 10, 7061-7068.	8.0	34
96	Atomically Dispersed Transition Metals on Carbon Nanotubes with Ultrahigh Loading for Selective Electrochemical Carbon Dioxide Reduction. Advanced Materials, 2018, 30, e1706287.	21.0	459
97	Layered oxides-LiNi1/3Co1/3Mn1/3O2 as anode electrode for symmetric rechargeable lithium-ion batteries. Journal of Power Sources, 2018, 378, 516-521.	7.8	24
98	High efficiency electrochemical reduction of CO ₂ beyond the two-electron transfer pathway on grain boundary rich ultra-small SnO ₂ nanoparticles. Journal of Materials Chemistry A, 2018, 6, 10313-10319.	10.3	92
99	Electrochemical CO ₂ Reduction with Atomic Ironâ€Dispersed on Nitrogenâ€Doped Graphene. Advanced Energy Materials, 2018, 8, 1703487.	19.5	369
100	Enhanced photocatalytic activity induced by sp3 to sp2 transition of carbon dopants in BiOCl crystals. Applied Catalysis B: Environmental, 2018, 221, 467-472.	20.2	58
101	Enhancing the photoresponse and photocatalytic properties of TiO2 by controllably tuning defects across {101} facets. Applied Surface Science, 2018, 434, 711-716.	6.1	23
102	Roomâ€Temperature Activation of Molecular Oxygen Over a Metalâ€Free Triazineâ€Decorated sp ² â€Carbon Framework for Green Synthesis. ChemCatChem, 2018, 10, 5331-5335.	3.7	3
103	Rheniumâ€Doped and Stabilized MoS ₂ Atomic Layers with Basalâ€Plane Catalytic Activity. Advanced Materials, 2018, 30, e1803477.	21.0	164
104	Stabilizing and Activating Metastable Nickel Nanocrystals for Highly Efficient Hydrogen Evolution Electrocatalysis. ACS Nano, 2018, 12, 11625-11631.	14.6	55
105	In Situ TEM: Theory and Applications. Springer Tracts in Modern Physics, 2018, , 381-477.	0.1	1
106	Ambipolar ferromagnetism by electrostatic doping of a manganite. Nature Communications, 2018, 9, 1897.	12.8	51
107	Graphene Oxideâ€Template Controlled Cuboidâ€Shaped Highâ€Capacity VS ₄ Nanoparticles as Anode for Sodiumâ€Ion Batteries. Advanced Functional Materials, 2018, 28, 1801806.	14.9	125
108	Monoâ€Atomic Fe Centers in Nitrogen/Carbon Monolayers for Liquidâ€Phase Selective Oxidation Reaction. ChemCatChem, 2018, 10, 3539-3545.	3.7	14

#	Article	IF	CITATIONS
109	Singleâ€Atom Catalysts: Atomically Dispersed Transition Metals on Carbon Nanotubes with Ultrahigh Loading for Selective Electrochemical Carbon Dioxide Reduction (Adv. Mater. 13/2018). Advanced Materials, 2018, 30, 1870088.	21.0	8
110	Surface Reorganization Leads to Enhanced Photocatalytic Activity in Defective BiOCl. Chemistry of Materials, 2018, 30, 5128-5136.	6.7	55
111	Evolution of Oxyhalide Crystals under Electron Beam Irradiation: An in Situ Method To Understand the Origin of Structural Instability. Inorganic Chemistry, 2018, 57, 8988-8993.	4.0	15
112	Coordination-supported organic polymers: mesoporous inorganic–organic materials with preferred stability. Inorganic Chemistry Frontiers, 2018, 5, 2018-2022.	6.0	5
113	Concurrent Synthesis of Highâ€Performance Monolayer Transition Metal Disulfides. Advanced Functional Materials, 2017, 27, 1605896.	14.9	35
114	Toward the Design of a Hierarchical Perovskite Support: Ultra-Sintering-Resistant Gold Nanocatalysts for CO Oxidation. ACS Catalysis, 2017, 7, 3388-3393.	11.2	40
115	Direct growth of MoS ₂ single crystals on polyimide substrates. 2D Materials, 2017, 4, 021028.	4.4	39
116	Hydroxyl-Dependent Evolution of Oxygen Vacancies Enables the Regeneration of BiOCl Photocatalyst. ACS Applied Materials & Interfaces, 2017, 9, 16620-16626.	8.0	176
117	Controlling Reaction Selectivity through the Surface Termination of Perovskite Catalysts. Angewandte Chemie, 2017, 129, 9952-9956.	2.0	19
118	Controlling Reaction Selectivity through the Surface Termination of Perovskite Catalysts. Angewandte Chemie - International Edition, 2017, 56, 9820-9824.	13.8	47
119	Coordinationâ€5upported Imidazolate Networks: Water―and Heatâ€5table Mesoporous Polymers for Catalysis. Chemistry - A European Journal, 2017, 23, 10038-10042.	3.3	3
120	In Situ Coupling Strategy for the Preparation of FeCo Alloys and Co ₄ N Hybrid for Highly Efficient Oxygen Evolution. Advanced Materials, 2017, 29, 1704091.	21.0	165
121	Sustainable synthesis of alkaline metal oxide-mesoporous carbons <i>via</i> mechanochemical coordination self-assembly. Journal of Materials Chemistry A, 2017, 5, 23446-23452.	10.3	22
122	Tailoring Nâ€Terminated Defective Edges of Porous Boron Nitride for Enhanced Aerobic Catalysis. Small, 2017, 13, 1701857.	10.0	60
123	Solid-state synthesis of ordered mesoporous carbon catalysts via a mechanochemical assembly through coordination cross-linking. Nature Communications, 2017, 8, 15020.	12.8	164
124	PdSe ₂ : Pentagonal Two-Dimensional Layers with High Air Stability for Electronics. Journal of the American Chemical Society, 2017, 139, 14090-14097.	13.7	509
125	Incorporating Rich Mesoporosity into a Ceria-Based Catalyst via Mechanochemistry. Chemistry of Materials, 2017, 29, 7323-7329.	6.7	45
126	Supper lattice structure transformation based on nonstoichiometric bismuth oxychloride. Microscopy and Microanalysis, 2017, 23, 1676-1677.	0.4	0

#	Article	IF	CITATIONS
127	Defect engineering in atomically-thin bismuth oxychloride towards photocatalytic oxygen evolution. Journal of Materials Chemistry A, 2017, 5, 14144-14151.	10.3	107
128	Exchange of Re and Mo atoms in MoS2 driven by Scanning Transmission Electron Microscopy. Microscopy and Microanalysis, 2017, 23, 1702-1703.	0.4	0
129	Realizing Selective and Aerobic Oxidation by Porous Transition-Metal-Salt@Ceria Catalyst. ChemistrySelect, 2016, 1, 1179-1183.	1.5	3
130	Synthesis of MCF-supported AuCo nanoparticle catalysts and the catalytic performance for the CO oxidation reaction. RSC Advances, 2015, 5, 100212-100222.	3.6	10
131	Mesoporous MnCeOx solid solutions for low temperature and selective oxidation of hydrocarbons. Nature Communications, 2015, 6, 8446.	12.8	241
132	<i>In-situ</i> optical transmission electron microscope study of exciton phonon replicas in ZnO nanowires by cathodoluminescence. Applied Physics Letters, 2014, 105, .	3.3	12
133	Bipolar Electrochemical Mechanism for Mass Transfer in Nanoionic Resistive Memories. Advanced Materials, 2014, 26, 3649-3654.	21.0	89
134	In Situ Transmission Electron Microscopy Investigation on Fatigue Behavior of Single ZnO Wires under High-Cycle Strain. Nano Letters, 2014, 14, 480-485.	9.1	62
135	In-situ TEM imaging of the anisotropic etching of graphene by metal nanoparticles. Nanotechnology, 2014, 25, 465709.	2.6	9
136	Exotic Reaction Front Migration and Stage Structure in Lithiated Silicon Nanowires. ACS Nano, 2014, 8, 8249-8254.	14.6	18
137	Filament growth dynamics in solid electrolyte-based resistive memories revealed by in situ TEM. Nano Research, 2014, 7, 1065-1072.	10.4	30
138	Real-time in situ TEM studying the fading mechanism of tin dioxide nanowire electrodes in lithium ion batteries. Science China Technological Sciences, 2013, 56, 2630-2635.	4.0	23
139	Recombination in SnO ₂ -Based Quantum Dots Sensitized Solar Cells: The Role of Surface States. Journal of Physical Chemistry C, 2013, 117, 10965-10973.	3.1	34
140	Recent development of studies on the mechanism of resistive memories in several metal oxides. Science China: Physics, Mechanics and Astronomy, 2013, 56, 2361-2369.	5.1	12
141	Dynamic nanomechanics of zinc oxide nanowires. Applied Physics Letters, 2012, 100, 163110.	3.3	9
142	Observation of intermediate template directed SiC nanowire growth in Si–C–N systems. Nanotechnology, 2012, 23, 415704.	2.6	3
143	The Piezotronic Effect of Zinc Oxide Nanowires Studied by In Situ TEM. Advanced Materials, 2012, 24, 4676-4682.	21.0	58
144	One-Pot Pyrolysis Method to Fabricate Carbon Nanotube Supported Ni Single-Atom Catalysts with Ultrahigh Loading. ACS Applied Energy Materials, 0, , .	5.1	19